XVIII. COMMUNICATIONS BIOPHYSICS*

Academic and Research Staff

Prof. D. B. Geselowitz†
Prof. P. R. Gray
Prof. H. B. Lee
Prof. W. T. Peake‡
Prof. W. A. Rosenblith
Prof. W. M. Siebert
Prof. R. Suzuki**
Prof. T. F. Weiss‡
Prof. H. Yilmaz††
Dr. J. S. Barlow‡‡
Dr. A. W. B. Cunningham
Dr. G. F. Dormont***
N. I. Durlach
Dr. H. Fischler†††
Dr. P. Gogan‡‡‡
Dr. R. D. Hall
Dr. N. Y. S. Kiang‡
Dr. R. R. Pfeiffer‡
Dr. R. Rojas-Corona
Dr. G. F. Songster
R. M. Brown‡
A. H. Crist‡
F. N. Jordan
D. P. Langbein‡

Graduate Students

J. A. Anderson
G. von Bismarck
L. D. Braida
S. K. Burns
H. S. Colburn
J. A. Freeman
J. J. Guinan, Jr.
D. K. Hartline
A. J. M. Houtsma
L. K. Krakauer
R. G. Mark
E. G. Merrill
P. J. Metz III
D. C. Milne
E. C. Moxon
M. Nahvi
P. H. O'Lague
D. J-M. Poussart
M. B. Sachs
M. M. Scholl
J. J. Singer
I. H. Thomae
M. L. Wiederhold

A. WAVEFORMS RECORDED EXTRACELLULARLY FROM NEURONS IN THE ANTEROVENTRAL COCHLEAR NUCLEUS OF THE CAT

In continuing studies of properties of single units in the cochlear nucleus, emphasis has been placed on the "oral pole" of the anteroventral cochlear nucleus. The anatomy of this region suggests that it may be the simplest to study from the standpoint of trying

---

*This work is supported by the National Institutes of Health (Grants MH-04737-05 and NB-05462-02), the Joint Services Electronics Programs (U.S. Army, U.S. Navy, and U.S. Air Force) under Contract DA 36-039-AMC-03200(E), the National Science Foundation (Grant GP-2495), and the National Aeronautics and Space Administration (Grant NsG-496).

†Visiting Associate Professor from the Moore School, University of Pennsylvania, NIH Fellow.

‡Also at Eaton-Peabody Laboratory, Massachusetts Eye and Ear Infirmary, Boston, Massachusetts.

**Visiting Assistant Professor from the Research Institute of Dental Materials, Tokyo Medical and Dental University, Tokyo, Japan.

††Visiting Professor from Arthur D. Little, Inc., Cambridge, Massachusetts.

‡‡Research Affiliate in Communication Sciences from the Neurophysiological Laboratory of the Neurology Service of the Massachusetts General Hospital, Boston, Massachusetts.

***Visiting Scientist from Centre d'Études de Physiologie Nerveuse, Paris, France.

†††From the Department of Electronics, Weizmann Institute of Science, Rehovoth, Israel.

‡‡‡Visiting Scientist from Université de Paris, Laboratoire de Neurophysiologie Comparée, Paris, France (IBRO Traveling Fellow).

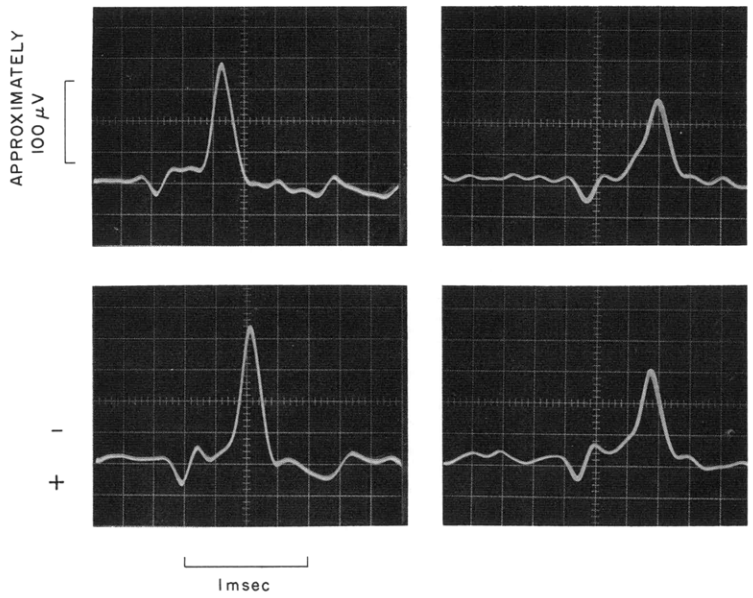

Fig. XVIII-1. Typical waveforms from neurons in the "oral pole" of the anteroventral cochlear nucleus. Although it is not shown here, relative amplitudes of the positive and negative components varies from unit to unit, presumably because of the electrode position relative to the cell body. Occasionally the positive component is quite small; however, it has not been difficult to detect its presence.

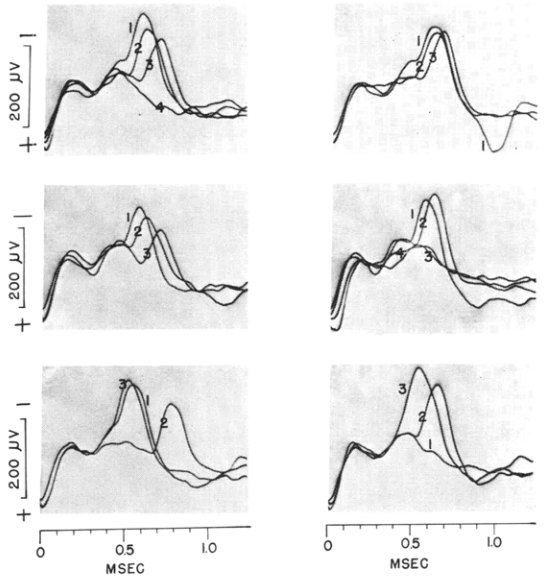

Fig. XVIII-2.

Superposed traces of series of 3 or 4 spikes. The numbers on each trace, in each set, indicate their temporal order. The times between spikes are not given (cf. Fig. XVIII-6). Each trace is synchronized to the positive component. The negative wave is composed of two components, the second of which occasionally fails to develop. Generally, as the time between spikes decreases, the delay of the second negative component as well as its probability of failure increases (cf. Fig. XVIII-6). These waveforms are in response to stimulation by continuous tone. The waveforms for spontaneous discharges are similar, but the probabilities of failure of the second negative component are much less. The failure of the second spike does not occur for all units; this failure may be a result of pressure applied to the cell body on account of the electrode's presence.

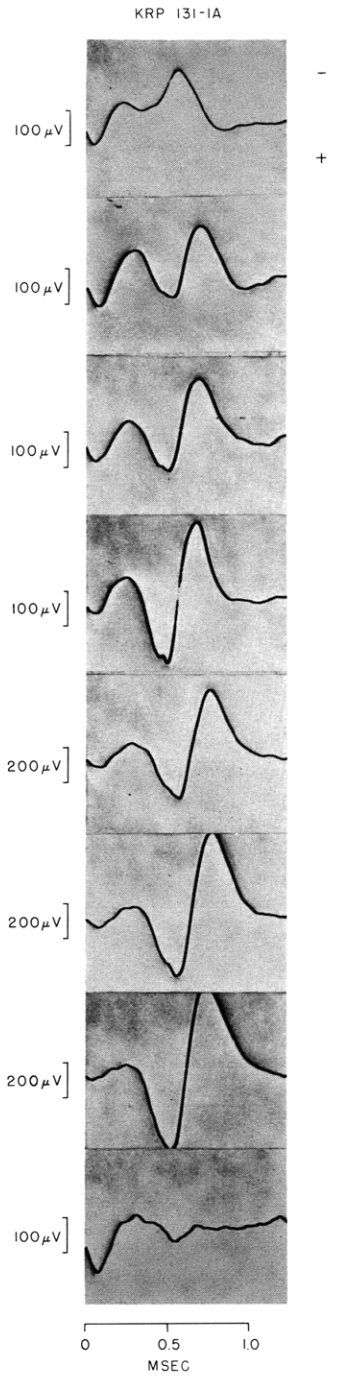

Fig. XVIII-3.
"Injury" sequences of spike discharge as the electrode is advanced (top to bottom). Each trace is synchronized to the positive component. Only the negative wave undergoes "injury." The positive wave is still present after the negative wave can no longer be developed.

to determine the functions of individual neurons. Two main features are: the relative homogeneity of this region with respect to anatomical description of the cells located there; and the fact that each of these cells receives single terminations from only a few – perhaps one to four – auditory nerve fibers.[1]

This report is limited to a brief description and interpretation of the extracellular wave shape recorded from neurons in this region. These single-neuron recordings were obtained by using metal-filled microelectrodes. We have found, however, that the wave shapes considered here can also be recorded extracellularly by using large fluid-filled (Ringer's solution) microelectrodes.

Figure XVIII-1 shows four spike potentials recorded from this region. The salient feature of these potentials – and that which makes them unique for cells in the cochlear nucleus – is the positive component preceding the more commonly encountered, extracellularly recorded negative component. That this waveform is actually composed of three separate components can be concluded from the data shown in Figs. XVIII-2 through XVIII-4. While the majority of recordings exhibit waveforms as shown in Fig. XVIII-1, often conditions are such that the negative wave separates into two components (Fig. XVIII-2). Also, when neurons in this region are subjected to injury, by advancement of an electrode, only the negative component is affected; the positive component is not (Fig. XVIII-3). Finally, in rare cases,

when these neurons discharge with pairs of spikes, the second spike does not have a positive component (Fig. XVIII-4).

We shall call the positive, the first negative, and the second negative components the P, A, and B components, respectively. Thus, we see P, A, B (Figs. XVIII-1 and

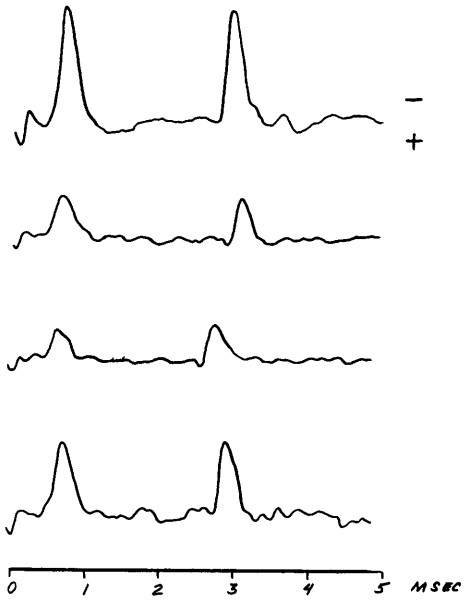

Fig. XVIII-4.

Tracings of waveforms of paired discharges. These pairs are infrequently encountered and relate, perhaps, to a pathology that will be handled elsewhere. Nevertheless, each of the second discharges in the pair does not have a positive component.

XVIII-2); P, A (Fig. XVIII-2); P (Fig. XVIII-3); and A, B (Fig. XVIII-4) combinations of components. Whether or not an A or a B component can occur in isolation has not yet been determined from our data.

Our present interpretation of the various components may be outlined as follows:

a. The P component is interpreted as a presynaptic event, detectable by the electrodes because of the large size of the synaptic endings; furthermore, the P components signify individual incoming spikes of all of the auditory-nerve fibers terminating on the neuron under study.

This interpretation is based, in part, on the following factors.

(i) The fact that the P component is not affected when the neuron undergoes "injury."

(ii) The delay (0.4-0.6 msec) between the P and the A component, which is reasonable for a synaptic delay between incoming spike and initiation of cell discharge.

(iii) The similarity between these positive potentials and those observed extracellularly from large synaptic endings in other preparations.[2,3,4a]

(iv) The consistency with the interpretation that the A and B components are postsynaptic – one that can be arrived at independently of this interpretation of the P spike.

(v) The fact that we have also recorded this type of waveform in the nucleus of the

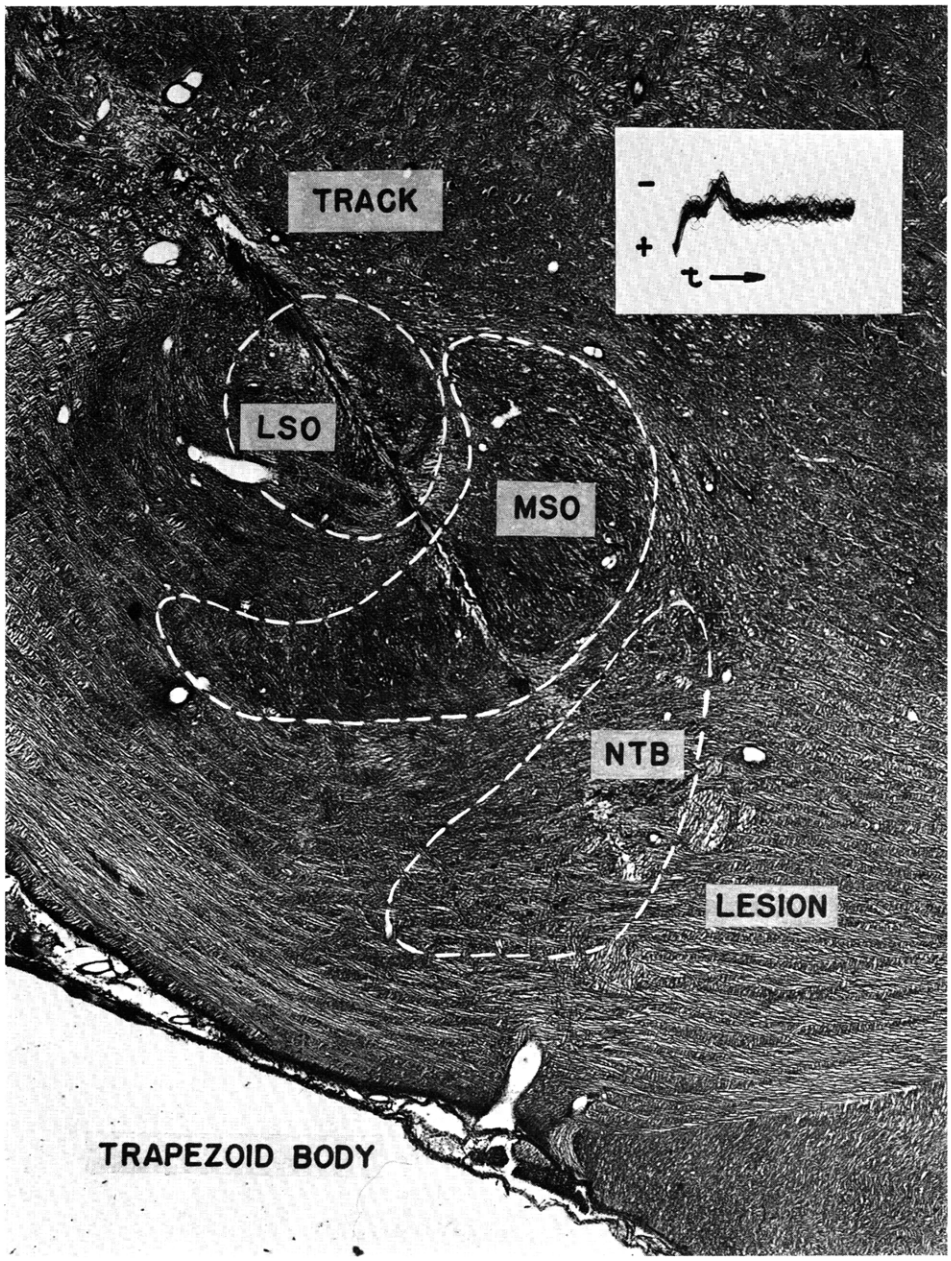

Fig. XVIII-5. Micrograph of electrode track leading to the nucleus of the trapezoid body. The neurons in this region have endings similar to those of neurons in the AVCN. Insert is a photograph of multiple tracings of waveforms recorded from the cell whose location was at the site of the lesion. The P component is obvious. LSO, lateral superior olivary nucleus; MSO, medial superior olivary nucleus; NTB, nucleus of the trapezoid body. Transverse section of left superior olivary complex.

trapezoid body in which there are neurons with similar large synaptic endings (Fig. XVIII-5).

b. The A and B components are interpreted as being postsynaptic events.

This interpretation is based, in part, on the following observations.

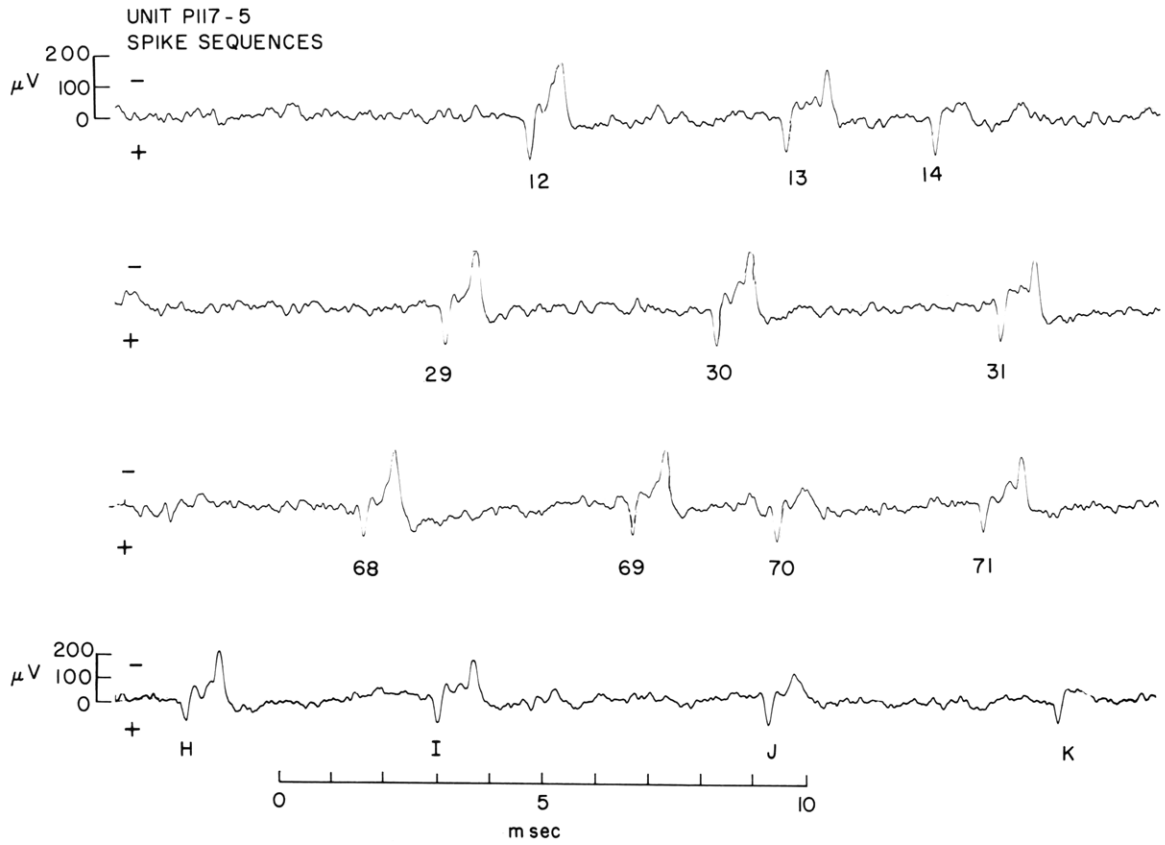

Fig. XVIII-6. Sequences of spikes illustrating the change in delay between the P and B (or A and B) components and the failure of the B component (cf. Fig. XVIII-2). These phenomena have been seen elsewhere (Fuortes et al.,[2] Li[6]). Perhaps the last spike shown consists only of a P component, which would indicate that the A component also failed to develop.

(i) The injury sequences demonstrated in Fig. XVIII-3 which are associated with injury of cell bodies.

(ii) The remarkable similarity to extracellular wave shapes recorded elsewhere, which exhibit this same A, B relation, and have been demonstrated to be postsynaptic events.[4b, 5]

(iii) The similarity between the failure of the B component, in cases of spikes occurring close to each other in time, for these cochlear nucleus neurons (Figs. XVIII-2

and XVIII-6) and the postsynaptic component failure observed in cortical[6] and motoneurons.[7]

(iv) The consistency with the interpretation that the P component is presynaptic.

The interpretation of the origin of the A and B components can be identical to that of Terzuolo and Araki (as well as others) for cases of spinal motoneurons. There appears to be no conflict with their interpretation – that the A component is the discharge of the initial segment (IS) of the cell structure and that the B component is the discharge of the soma-dendrite (SD) complex. It is possible, however, that the A component is not an IS discharge but rather an excitatory postsynaptic potential (EPSP).

Our present explanation of the polarities of the various components as monitored by extracellular electrodes is essentially that of Takeuchi and Takeuchi[2] for the P component, and of Terzuolo and Araki[5] for the A and B components. Further details of these waveforms, as well as other properties of these neurons, will be considered elsewhere.

R. R. Pfeiffer, W. B. Warr

[Dr. W. B. Warr is a Research Associate in Otolaryngology at the Massachusetts Eye and Ear Infirmary, Boston, Massachusetts.]

References

1. S. Rámon y Cajal, Histologie du système nerveaux de l'homme et des vertebres, Vol. 1 (Maloine, Paris, 1909), pp. 781-787.

2. A. Takeuchi and N. Takeuchi, "Electrical Changes in Pre- and Postsynaptic Axons of the Giant Synapse of Loligo," J. Gen. Physiol. 45, 1181-1193 (1962).

3. J. I. Hubbard and R. F. Schmidt, "An Electrophysiological Investigation of Mammalian Motor Nerve Terminals," J. Physiol. (Lond.) 166, 145-167 (1963).

4. J. C. Eccles, "The Physiology of Synapses" (Springer-Verlag, Berlin, 1964), (a) pp. 122-127; (b) Chapters VII and X.

5. C. A. Terzuolo and T. Araki, "An Analysis of Intra- versus Extracellular Potential Changes Associated with Activity of Single Spinal Motoneurons, Ann. N. Y. Acad. Sci. 94, 547-558 (1961).

6. C. L. Li, "Cortical Intracellular Synaptic Potentials," J. Cell. Comp. Physiol. 58, 153-167 (1961).

7. M. G. F. Fuortes, K. Frank, and M. C. Becker, "Steps in the Production of Motoneuron Spikes," J. Gen. Physiol. 40, 735-752 (1957).

B. THE FLUCTUATION OF EXCITABILITY OF A NODE OF RANVIER

1. Introduction

Fluctuations of the excitability of a node of Ranvier from a peripheral nerve fiber were first reported by Blair and Erlanger,[1] studied by Pecher,[2] and more recently by Verveen[3,4] and Derksen.[5] Following is a brief account of some experiments dealing with this phenomenon which we have recently performed.[6]

The workers cited above observed that a node of Ranvier, when excited by identical rectangular depolarizing current pulses (of duration τ and intensity i) exhibits fluctuations of two types:

(i) In the vicinity of the threshold, a response is obtained in only a fraction of the trials.

(ii) The latency of the response fluctuates from trial to trial.

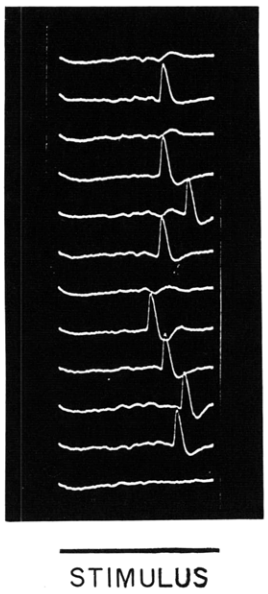

Fig. XVIII-7.

Samples of repetitive trials. A fiber is stimulated at a rate of 0.5 sec^{-1} with identical current stimuli of near-threshold intensity. Each record starts with the onset of the stimulus, which is represented by a heavy bar. The observed delay of the response consists of two terms: first, a delay produced by the "excitation process" at the locus of stimulation, second, a delay caused by the finite conduction velocity of the fiber (in this case over a distance of 7 cm). The second delay can be considered as a constant for our purpose. In the sequel, "latency" is to be equated with the first delay.

These two types of fluctuation are illustrated by the data presented in Fig. XVIII-7. It appears that for rates of stimulation lower than 0.5 sec^{-1}, the firings can be described as a set of Bernoulli trials, that is, the responses to successive trials appear to be mutually independent and to occur with a fixed probability.

Excised sciatic-peroneal nerve preparations from Rana pipiens were used in these experiments. Action potentials were recorded from fibers in the phalangeal branches of the nerve by means of gross electrodes. The signal-to-noise ratio of the recorded signals and the amplitude of the artifact were such that the latency could be measured with a standard error of 20 μsec by means of a level-crossing device. The preparation was stimulated proximally with tripolar tungsten or silver silver-chloride electrodes. Throughout a sequence of successive trials, the stimuli could be maintained constant within 0.1% of a prescribed value, both in intensity and in duration. The temperature of the preparation was between 18°C and 22°C and was kept within 0.1°C of a fixed value during the course of an experiment. The responses of 63 single fibers were obtained.

2. Intensity Function

For a given stimulus duration τ, it has been found that a Gaussian distribution, with mean $\bar{i}_\tau$ and standard deviation σ_τ, could be fitted to the experimental curve relating the average number of firings to the intensity i of the stimulus[2,3] (the intensity function). The threshold is defined as $\bar{i}_\tau$.

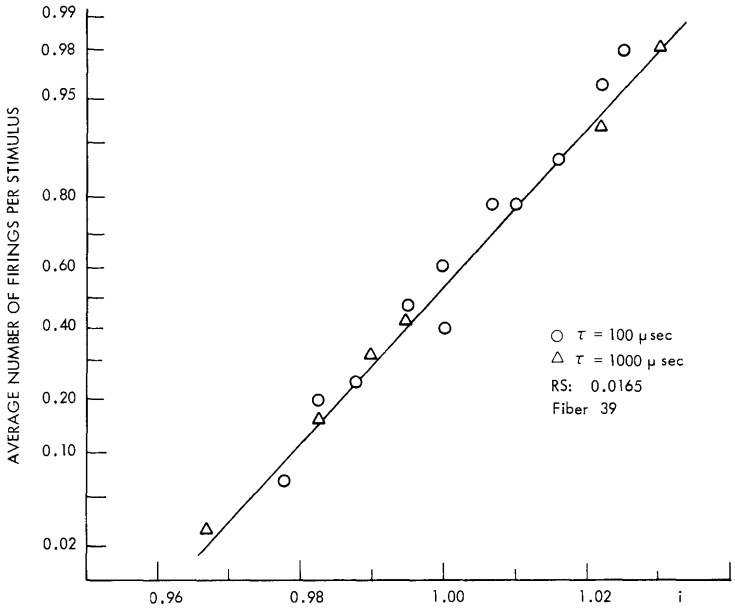

Fig. XVIII-8. Intensity Function, plotted on a normal scale for two durations of the stimulus. The corresponding threshold is normalized to 1.0 in both cases.

Figure XVIII-8 shows a measurement of the intensity function obtained in the present study. The vertical scale is such as to map a Gaussian distribution into a straight line whose slope is inversely related to the standard deviation. The figure presents data obtained for τ = 100 μsec and τ = 1000 μsec. Each point corresponds to the relative frequency of response to 100 successive, identical stimuli presented at the rate of 0.5 sec^{-1}. For both values of τ, $\bar{i}_{100}$ and $\bar{i}_{1000}$ have been normalized to 1.0 and i correspondingly transformed. These data support the hypothesis that the intensity function can be described as a Gaussian distribution function. The superposition of the experimental points for both values of τ illustrates the invariance of the quantity $(\sigma_\tau/\bar{i}_\tau)$, called "Relative Spread" (RS). This is in agreement with Verveen,[3] who has reported such invariances over the 200-2000 μsec range of τ, but at variance with the results of DeBecker[7] (for τ = 200 and 4000 μsec) which were obtained, however, on a different preparation.

3. Latency Distribution

The necessity of using low rates of stimulation, coupled with the limited time over which a preparation yields reproducible observations (typically a few hours), has restricted the number of samples from which the distribution of the latency could be estimated. For this reason, only the mean and standard deviations were considered quantitatively.

Qualitatively, as the intensity of the stimulus is increased, the mean, M, and the standard deviation, S, of the distribution of latency decrease, while the distribution changes from highly unsymmetrical, with a positive third central moment, to more symmetrical.

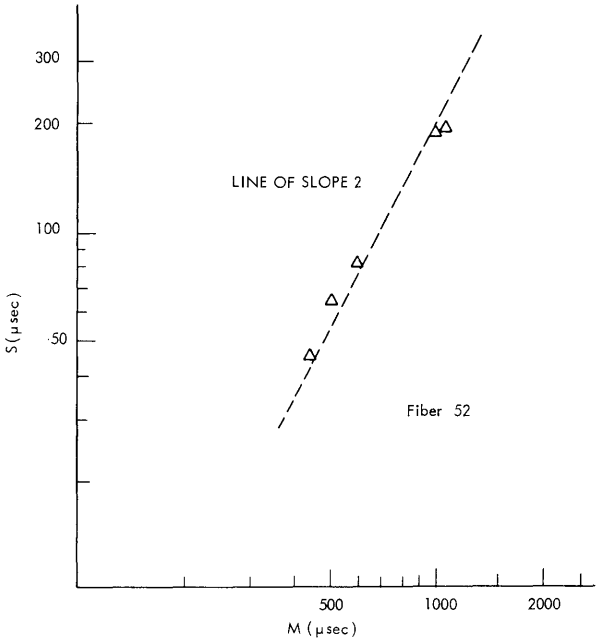

Fig. XVIII-9.

Standard deviation of the latency, S, as a function of the mean, M, of the latency in log-log coordinates.

Quantitatively, one observes an interesting relation between S and M, illustrated in Fig. XVIII-9. S appears to be linearly related to M^2 over a range of stimulus intensity of $0.5\bar{i}_T < i < 2\bar{i}_T$. Unfortunately, the type of preparation that was used is not suited to the estimation of latency distributions outside of the above-mentioned range of intensity.

A similar dependence of S on M has recently been reported by Verveen. A Monte-Carlo simulation[4,8] of a mathematical model of the fluctuation of excitability has also produced a similar functional relationship between S and M for the range of i given above. [The reader is referred to the original paper of Ten Hoopen and his co-workers[8] and to the author's thesis[6] for a description of that model.] Data such as those presented

in Fig. XVIII-9 were compared with the results of the simulation. From this comparison, an estimate of the upper cutoff frequency of the power spectrum of the "membrane noise" was obtained.[6]

4. Remarks

Slow fluctuations (e.g., with time courses of 1 minute or more) in the measured values of both the threshold and the RS of a node of Ranvier were frequently observed in this investigation. It has not yet been possible to ascertain whether or not these fluctuations were intrinsic properties of the membrane. In spite of the care in the control of those factors of known influence on the stability of the preparation, experimental artifacts are not ruled out as a source of such slow fluctuations. For this reason, two of our experimental techniques are currently being re-examined. Liquid-stimulating electrodes are being investigated in order to eliminate possible changes in the coupling between the epineurium and the metal electrodes imbedded in mineral oil. The possible effect of coupling between a given fiber whose responses are observed and its neighbors at the locus of stimulation will be examined soon. An optically coupled stimulator has been designed in order to be able to both stimulate and record on a phalangeal branch with a negligible artifact. It will thus be possible to monitor the responses of all excited fibers of a branch, and investigate the effect of interfiber coupling.

If it can be shown that such slow fluctuations are properties of the membrane, the current form of mathematical models for the excitability of a node in terms of a stationary random process may have to be revised.

D. J-M. Poussart

References

1. E. A. Blair and J. Erlanger, "A Comparison of the Characteristics of Axons through Their Individual Electrical Responses," Am. J. Physiol. 106, 524-564 (1933).
2. C. Pecher, "La fluctuation d'excitabilité de la fibre nerveuse," Arch. Int. Physiol. 49, 129-152 (1939).
3. A. A. Verveen, "Fluctuations in Excitability," Netherlands Central Institute for Brain Research, Drukkerij Holland N. V., Amsterdam, 1961.
4. A. A. Verveen and H. E. Derksen, "Fluctuations in Membrane Potentials of Axons and the Problem of Coding," Kybernetik 2, 4 ht (1965).
5. H. E. Derksen, "Axon Membrane Voltage Fluctuations," Acta Physiol. Pharmacol. Neerl. 13, 373-466 (1965).
6. D. J-M. Poussart, "Measurements of Latency Distributions in Peripheral Nerve Fibers," S. M. Thesis, Department of Electrical Engineering, Massachusetts Institute of Technology, 1965.
7. J. C. DeBecker, "Fluctuations in Excitability of Single Myelinated Nerve Fibers," Separatum Experientia 20, 553 (1964).
8. M. Ten Hoopen, A. Den Hertog, and H. A. Reuver, "Fluctuations in Excitability – A Model Study," Kybernetik 2, 1 ht, 1-8 (1963).

C. BIOELECTRIC POTENTIALS IN AN INHOMOGENEOUS VOLUME CONDUCTOR

Electric potentials of cardiac origin can readily be recorded at the surface of the body. A fundamental problem in electrocardiography is to relate these potential differences to their sources in the heart muscle. In this report an attempt is made to provide a formal analysis of this problem. While the emphasis is on the electrocardiographic problem, the basic problem is one of the distribution of action currents in an inhomogeneous volume conductor, and the results should be applicable to potentials arising from nerve, as well as from muscle.

The solution to the problem depends, of course, on the electrical properties of body tissues. These properties have been studied quite extensively[1,2] and several important conclusions can be drawn. First, electromagnetic wave effects can be neglected[3] and the problem is thus a quasi-static one. Hence if $\bar{E}$ is the electric field intensity at a point in the body, and V is the electric scalar potential, at each instant

$$\bar{E} = -\nabla V. \tag{1}$$

A second conclusion is that for the current densities present as a result of action potentials, body tissues are linear,[1] and the current density, $\bar{J}$, is linearly related to the field $\bar{E}$. Furthermore, the capacitive component of tissue impedance is negligible at frequencies of interest to electrocardiography[2] (below 1 kHz), and there is also evidence that pulses with rise times of approximately 1 μsec suffer negligible distortion.[4] If tissue conductivity is designated g, then

$$\bar{J} = g\bar{E} \tag{2}$$

for regions where there are no bioelectric sources.

In Eq. 2 it is assumed that tissues are isotropic, at least if g is to be a scalar quantity. Evidence on this point is incomplete. Clearly, individual muscle fibres are not isotropic, but apparently to a good approximation, for the present purposes, a region of tissue is effectively isotropic because of randomness in the orientation of cells,[1] and can be assigned a bulk conductivity that is isotropic.

As a consequence of these properties of body tissues, the currents at any instant depend only on the values of the sources at that instant. Formally, we can represent the sources by a distribution of impressed current densities, $\bar{J}^i$. Later we shall attempt to relate $\bar{J}^i$ to electrical activity associated with the plasma membranes of the active cells. Equation 2 can be modified to include active regions as follows:

$$\bar{J} = g\bar{E} + \bar{J}^i. \tag{3}$$

If the accumulation of charge in any region is to be zero, we have the additional relation

$$\nabla \cdot \bar{J} = 0 \tag{4}$$

which can be combined with Eqs. 1 and 3 to give

$$\nabla \cdot g\nabla V = \nabla \cdot \bar{J}^i. \tag{5}$$

Conductivities of the various tissue masses in the thorax are quite similar. Major exceptions are blood, which has a much higher conductivity than the average, and lung, whose conductivity may vary considerably over the respiratory cycle. It is reasonable, then, to divide the body into homogeneous regions, in each of which the conductivity is constant.

Let the surface S_j separate regions of conductivity g' and g", and let $d\bar{S}_j$ be a differential element of the area of this surface. Adopt the convention that $d\bar{S}_j$ is directed from the primed region to the double primed one. Since the current must be continuous across each boundary,

$$g'\nabla V' \cdot d\bar{S}_j = g''\nabla V'' \cdot d\bar{S}_j. \tag{6}$$

Furthermore, the potential is also continuous at each boundary. Hence

$$V'(S_j) = V''(S_j). \tag{7}$$

Our problem, then, is to determine V from a knowledge of $\bar{J}^i$, using Eqs. 5, 6, and 7. More particularly in electrocardiography, our problem is to determine $\bar{J}^i$, given V on the body surface. Similarly, in studying action potentials from nerve or cardiac muscle with microelectrodes, the problem is often to determine J^i from a knowledge of the potential difference between the microelectrode and a reference electrode. This "inverse" problem will be discussed further.

Let dv be an element of volume of a homogeneous region, and ψ and ϕ be two functions that are well behaved in each region. Green's theorem[5] then states that

$$\sum_j \int_{S_j} \left[g'(\psi'\nabla\phi' - \phi'\nabla\psi') \; -g''(\psi''\nabla\phi'' - \phi''\nabla\psi'')\right] \cdot d\bar{S}_j = \sum_v \int_v \left[\psi\nabla \cdot g\nabla\phi - \phi\nabla \cdot g\nabla\psi\right] dv. \tag{8}$$

Three cases are of interest and they will be discussed separately.

Case I

Let

$$\phi = V \tag{9}$$

$$\nabla^2\psi = 0 \tag{10a}$$

$$\psi'(S_j) = \psi''(S_j). \tag{10b}$$

Then from Eqs. 5, 6, and 7,

$$-\sum_j \int_{S_j} V(g'-g'')\nabla\psi \cdot dS_j - \int_{S_o} gV\nabla\psi \cdot d\vec{S}_o = \sum \int_v (\psi\nabla\cdot\vec{J}^i - V\nabla g\cdot\nabla\psi)\, dv, \tag{11}$$

where S_o is the external surface of the body, and the summation j is over internal surfaces of discontinuity. Our assumption is that ∇g is zero in each region, that is, each region is homogeneous. Hence the last term vanishes. The first term on the right can be transformed as follows:

$$\int \nabla\cdot(\vec{J}^i\psi)\, dv = \int \psi\vec{J}^i \cdot d\vec{S} = \int (\vec{J}^i\cdot\nabla\psi + \psi\nabla\cdot\vec{J}^i)\, dv.$$

If $\vec{J}^i$ vanishes on S, then

$$\int \psi\nabla\cdot\vec{J}^i\, dv = -\int \vec{J}^i\cdot\nabla\psi\, dv \tag{12}$$

and Eq. 11 becomes

$$\int_{S_o} gV\nabla\psi\cdot dS_o + \sum_j \int_{S_j} (g'-g'')V\nabla\psi\cdot dS_j = \int \vec{J}^i\cdot\nabla\psi\, dv. \tag{13}$$

Let $\vec{P}$ be a fictitious volume distribution of sources in a homogeneous conductor, g_o, chosen so that V on S_o remains the same. Then

$$\int_{S_o} g_o V\nabla\psi\cdot dS_o = \int \vec{P}\cdot\nabla\psi\, dv. \tag{14}$$

Now consider that the conductivity at the body surface is constant and let its value be g_o. From Eqs. 13 and 14,

$$g_o \int_{S_o} V\nabla\psi dS_o = \int \vec{P}\cdot\nabla\psi\, dv = \int \vec{J}^i\cdot\nabla\psi\, dv - \sum_j \int_{S_j} (g'-g'')V\nabla\psi\cdot d\vec{S}_j. \tag{15}$$

Equation 15 is the basic result of Case I. It is valid for each choice of ψ satisfying Eqs. 10a and 10b. Note that to evaluate the integral on the left, only a knowledge of the surface potential distribution is required. The fictitious, or equivalent, source distribution, $\vec{P}$, is not uniquely determined. Indeed there is an infinite number of choices of $\vec{P}$ that will satisfy Eq. 14. The multipole expansion[6] provides a canonical description of $\vec{P}$. In this representation $\vec{P}$ consists of singularities at a single point.

The various terms of the multipole expansion can be obtained by letting

$$\psi_{nm} = \left(2-\delta_m^o\right)\frac{(n-m)!}{(n+m)!}\, r^n P_n^m(\cos\theta)\, e^{im\phi}, \tag{16}$$

where (r, θ, ϕ) are the coordinates of a point in space relative to the origin at the location

of the multipoles, P_n^m is an associated Legendre polynomial, and δ_m^o is the Kronecker delta which is unity for m = 0 and zero for other values of m. Both n and m are non-negative integers, and m is less than or equal to n. Note that ψ_{nm} satisfies Eqs. 10a and 10b.

In particular, the multipole components a_{nm} and b_{nm} are given by

$$a_{nm} + ib_{nm} \equiv \int \vec{P} \cdot \nabla\psi_{nm}\, dv. \tag{17}$$

Therefore

$$a_{nm} + ib_{nm} = \int g_o V \nabla\psi_{nm} \cdot d\vec{S}_o = \int \vec{J}^i \cdot \nabla\psi_{nm}\, dv - \sum_j \int_{S_i} (g'-g'')V\nabla\psi_{nm} \cdot d\vec{S}_j. \tag{18}$$

Thus the multipole components can be evaluated from a knowledge of the surface potential distribution and can be related to the actual source distribution, if known. The monopole term a_{oo} vanishes. When n is 1, we have the dipole term for which

$$\psi_{10} = r \cos\theta = z$$

$$\psi_{11} = r \sin\theta\, e^{im\phi} = x + iy.$$

If the dipole moment, $\vec{p}$, is defined as

$$p \equiv ia_{11} + jb_{11} + ka_{10}, \tag{19}$$

then

$$\vec{p} = \int g_o V d\vec{S}_o = \int \vec{J}^i dv - \sum_j \int_{S_i} (g'-g'')V d\vec{S}_j = \int \vec{P} dv. \tag{20}$$

The five components of the quadrupole are obtained by letting n = 2, and can be evaluated in similar fashion. Note that it is impossible to distinguish two equivalent distributions whose multipole expansions are identical.

Case II

Let us retain Eqs. 9 and 10b, but change Eq. 10a so that

$$\psi = \frac{1}{r}, \tag{21}$$

where r is the distance from an arbitrary point to the element of volume or area. The derivation then proceeds in a very similar manner except that in Eq. 11 we must retain the term involving $\nabla^2\psi$. Thus

$$-\sum_j \int_{S_j} V(g'-g'')\, \nabla\left(\frac{1}{r}\right) \cdot dS_j - \int_{S_o} gV\nabla\left(\frac{1}{r}\right) \cdot dS_o = \int_v \left[\frac{1}{r}\nabla \cdot \vec{J}^i - Vg\nabla^2\left(\frac{1}{r}\right)\right] dv. \tag{22}$$

The first term on the right can be transformed by using Eq. 12. The second term can be evaluated to give

$$\int_v gV\nabla^2\left(\frac{1}{r}\right) dv = -4\pi gV, \tag{23}$$

where g and V are evaluated at r = 0, that is, the arbitrary point. Therefore

$$\psi\pi gV = \int_v \vec{J}^i \cdot \nabla\left(\frac{1}{r}\right) dv - \sum_j \int_{S_j} V(g'-g'')\nabla\left(\frac{1}{r}\right)\cdot dS_j - \int_{S_o} gV\nabla\left(\frac{1}{r}\right)\cdot dS_o. \tag{24}$$

This equation is the basis of an iterative technique[7] for the solution of Eq. 5, subject to the boundary conditions (6) and (7). If each side of the equation is divided by $4\pi g$, then the first term on the right can be interpreted as the potential that would exist at a point in an unbounded homogeneous conductor of conductivity g resulting from a current source distribution J^i. The next two terms can be similarly interpreted in terms of double layers at the discontinuities.

Case III

Return to Eq. 8 and let

$$\begin{aligned} g\phi &= V \\ \psi &= \frac{1}{r}. \end{aligned} \tag{25}$$

Then, with the use of Eqs. 5 and 7,

$$-\sum_j \int_{S_i} \frac{1}{r}(\vec{E}'-\vec{E}'')\cdot d\vec{S}_j - \int_{S_o} \frac{1}{r}\vec{E}''\cdot d\vec{S}_o = \sum \int_v \left[\frac{1}{rg}\nabla\cdot\vec{J}^i - V\nabla^2\left(\frac{1}{r}\right)\right] dv. \tag{26}$$

The two terms of the right-hand integral can be transformed by using Eqs. 12 and 23. The terms on the left of the equality sign can be rearranged as follows. From Eq. 6,

$$g'E'_n = g''E''_n. \tag{27}$$

Here the subscript n indicates the normal component, that is, in the direction of $d\vec{S}_j$. Define

$$E_j \equiv \frac{1}{2}(E'_n+E''_n) = \frac{1}{2}E'_n(1+g'/g''). \tag{28}$$

Then

$$E'_n - E''_n = E'(1-g'/g'') = 2E_j\frac{g''-g'}{g''+g'} \tag{29}$$

and Eq. 26 becomes

$$-\sum_j \int_{S_j} \frac{2E_j}{r} \frac{g'' - g'}{g'' + g'} \, dS_j + \int_{S_o} \frac{2E_j}{r} \, dS_o = -\int \frac{1}{g} \vec{J}^i \nabla\left(\frac{1}{r}\right) dv + 4\pi V$$

or

$$V = \int \frac{1}{4\pi g} \vec{J}^i \nabla\left(\frac{1}{r}\right) dv + \sum_j \int_{S_j} \frac{2\epsilon E_j}{4\pi\epsilon r} \frac{g' - g''}{g' + g''} \, dS_j + \int_{S_o} \frac{2\epsilon E_j}{4\pi\epsilon r} dS_o. \tag{30}$$

Equation 30 can be interpreted in a manner analogous to that used for Eq. 24. The first term on the right again gives the potential that would exist at an arbitrary point in an unbounded medium of conductivity g resulting from current sources $\vec{J}^i$. The second and last terms represent the potential in an unbounded medium of permittivity ϵ arising from a surface charge distribution, ω_j, given by

$$\omega_j = 2\epsilon E_j \frac{g' - g''}{g' + g''}. \tag{31}$$

Note that the last term is a special case in which $g'' = 0$, and the potential is independent of the value chosen for ϵ.

E_j can be looked upon as the normal component of the electric field that would exist at the point in question if the surface charge, ω_j, at the point were not present. This interpretation follows from the fact that if E_o is the normal component of the field attributable to all other sources, then

$$E'_n = E_o - \delta E$$

$$E''_n = E_o + \delta E,$$

where

$$\delta E = \frac{\omega_j}{2\epsilon},$$

in order to satisfy the boundary condition

$$E''_n - E'_n = \omega_j/\epsilon. \tag{32}$$

Note that Eq. 32 is consistent with Eqs. 29 and 31.

Equation 30 can also be used as the basis of an interative technique to solve the boundary value problem.[8] The potential, and hence E_j, can be determined from the first integral on the right by taking ω_j initially equal to zero. Next, ω_j can be evaluated from Eq. 31, and E_j recalculated from Eq. 30. The process can be repeated until the values of ω_j stabilize.

Relation to Membrane Activity

Thus far, the myocardium has been represented by a distribution of current sources, $\bar{J}^i$, in a uniform conductor. It is of interest to relate $\bar{J}^i$ to electrical activity associated with cell membranes. We shall assume that the interior of each cell is a passive conductor of conductivity g_i, while the intracellular fluid is a passive conductor of conductivity g_e. The membranes are sites of complex electrical activity; they will be excluded when applying Green's theorem.

Return to Case II. Equation 22 must now be modified to exclude membranes in the myocardial region. Since all remaining regions are passive, the term involving J^i disappears. Conversely on the left-hand side of Eq. 22 new terms appear involving integrations over the internal surface, S_{mi}, and external surfaces, S_{me}, of each plasma membrane. The net result in Eq. 25 is thus to replace the volume integral involving J^i with surface integrals over membranes as follows:

$$\int \bar{J}^i \cdot \nabla\left(\frac{1}{r}\right) dv = \int_{S_{mi}} g_i\left[\frac{1}{r_i}\nabla V_i - V_i \nabla\left(\frac{1}{r_i}\right)\right] \cdot d\bar{S}_{mi} - \int_{S_{me}} g_e\left[\frac{1}{r_e}\nabla V_e - V_e \nabla\left(\frac{1}{r_e}\right)\right] \cdot d\bar{S}_{me}, \tag{33}$$

where r_i and r_e are distances from an arbitrary point outside the heart region to the elements dS_{mi} and dS_{me}, respectively, and V_i and V_e are the corresponding potentials.

Following Plonsey[9] we shall assume that the transverse membrane current, J_m, taken positive outward, is

$$-J_m = g_i(\nabla V_i)_n = g_e(\nabla V_e)_n. \tag{34}$$

Furthermore, if the membrane thickness, m, is small compared with r, then

$$\frac{dS_{mi}}{r_e} - \frac{dS_{me}}{r_i} \approx dS_m\left(\frac{1}{r_e} - \frac{1}{r_i}\right) \approx d\bar{S}_m \cdot m\nabla\left(\frac{1}{r}\right). \tag{35}$$

To the same order of approximation,

$$\nabla\left(\frac{1}{r_i}\right) \cdot d\vec{S}_{mi} = \nabla\left(\frac{1}{r_e}\right) \cdot d\vec{S}_m = \nabla\left(\frac{1}{r}\right) \cdot d\vec{S}_m. \tag{36}$$

Hence

$$\int \vec{J}^i \cdot \nabla\left(\frac{1}{r}\right) dv = \int_{S_m} [J_m m - g_i V_i + g_e V_e] \nabla\left(\frac{1}{r}\right) \cdot d\bar{S}_m = \int (J_m m - g_i V_i + g_e V_e)\, d\Omega, \tag{37}$$

where $d\Omega$ is the solid angle subtended by dS_m. Plonsey has pointed out that generally

$$g_e|V_e - V_i| \gg mJ_m. \tag{38}$$

For example, let $g_e = g_i = 10^{-3}$ mho/cm, $|V_i - V_e| = 10$ mv, and m = 1000 Å. Then

$g_e(V_i-V_e)/m$ is approximately 1000 ma/cm^2, which is much larger than observed values of J_m. With this approximation, then, for $g_e = g_i$,

$$\bar{J}^i\,dv = (g_eV_e-g_iV_i)d\bar{S}_m, \tag{39}$$

and each element of membrane area acts as a current dipole source whose moment is related to the transmembrane potential.

Note that when the cell is in its resting state V_e and V_i are constant over S_m. In this circumstance, the integral in Eq. 37 taken over the entire cell boundary becomes

$$(g_eV_e-g_iV_i)\oint d\Omega = 0. \tag{40}$$

Thus a uniform potential along both sides of the membrane produces no external fields. Consequently, calculations involving Eqs. 24 and 37 can be done equivalently by considering departures of $\left(V_e - \frac{g_i}{g_e}V_i\right)$ from its resting value. As a corollary, if a region of membrane is uniformly depolarized, it is sometimes convenient to use Eq. 40 and replace the active region by complementary regions that complete a closed surface and have an opposite dipole moment.

When Eq. 37 is substituted in Eq. 24, the result is

$$4\pi gV = \int_{S_m}(J_m m-g_iV_i+g_eV_e)\,d\Omega - \sum_j \int_{S_j} V(g'-g'')\,\nabla\left(\frac{1}{r}\right)dS_j - \int_{S_o} gV\nabla\left(\frac{1}{r}\right)dS_o. \tag{41}$$

The first integral is the source term, the second integral accounts for inhomogeneities in the volume conductor, and the third integral accounts for the external boundary. While the equation cannot be directly integrated to obtain solutions, since the last two integrals require a knowledge of the potentials we are seeking, it does provide insight into the nature of the solution. As indicated above, iterative techniques can be used to obtain solutions with the aid of digital computers.

Equation 41 was obtained from Case II by excluding the membrane from the region of integration. Case III can be treated in an identical manner. The result is

$$4\pi V = \int\left[\left(\frac{1}{g_e}-\frac{1}{g_i}\right)\frac{\vec{J}_m}{r} + (V_e-V_i)\nabla\left(\frac{1}{r}\right)\right]\cdot dS_m + \sum_j \int_{S_j}\frac{2E_j}{r}\frac{g'-g''}{g'+g''}\,dS_j + \int_{S_o}\frac{2E_j}{r}\,dS_o. \tag{42}$$

If $g_i = g_e$, then the first integral in Eq. 41 is just g times the first integral in Eq. 42.

In electrocardiography the major discontinuities are those at the inner and outer surfaces of the heart, for example, at the interface with the intracavitary blood mass and with the lungs. The changing impedance of the lungs during respiration is probably responsible for the respiratory variations observed in the electrocardiogram.

Note that the first integrals in Eqs. 41 and 42 involve the potential and its normal derivative over a surface bounding a region containing no sources. These two functions are not independent. In practice, only a portion of a cell membrane is actively depolarized at any instant. Strictly speaking, the presence of transverse current, J_m, at nonactive membrane sites must also be taken into account in evaluating the fields everywhere in the present formulations. To a first approximation, only potentials and currents at active membrane sites need be considered.

Equation 41 or 42 should also be applicable for determining the potential at an extracellular microelectrode. In this case effects of inhomogeneities can be neglected to a first approximation if they are sufficiently far removed from the recording electrodes and the active areas.

Either equation, then, provides an implicit expression for the potentials throughout an inhomogeneous volume conductor, given a knowledge of membrane potentials and currents at all active sites at any instant of time. In practice, the transverse currents at adjacent membrane sites will result in the spread of depolarization. A knowledge of the voltage current relation at the membrane should enable one to calculate the spread of excitation. This topic is beyond the scope of the present treatment.

D. B. Geselowitz

References

1. H. P. Schwan and C. F. Kay, "Specific Resistance of Body Tissues," Circulation Research 4, 664-670 (1956).
2. H. P. Schwan and C. F. Kay, "Capacitive Properties of Body Tissues," Circulation Research 5, 439-443 (1957).
3. D. B. Geselowitz, "The Concept of an Equivalent Cardiac Generator," Biomedical Sciences Instrumentation, Vol. I (Plenum Press, New York, 1963).
4. S. A. Briller, D. B. Geselowitz, G. K. Danielson, C. R. Joyner, and S. D. Arlinger, "Use of a Current Probe in the Evaluation of Failure of Artificial Pacemakers," Proceedings of 17th Annual Conference on Engineering in Medicine and Biology, Cleveland, Ohio, November, 1964, Vol. 6, p. 120.
5. W. P. Smythe, Static and Dynamic Electricity (McGraw-Hill Book Company, New York, 1950), pp. 48-58; 129-138.
6. D. B. Geselowitz, "Multipole Representation for an Equivalent Cardiac Generator," Proc. IRE, 48, 75-79 (1960).
7. R. Barr, T. C. Pilkington, J. P. Boineau, and M. S. Spach, "Correlation between Body Surface Potential Distribution and Ventricular Excitation," Proc. 18th ACEMB, Philadelphia, November 1965, Vol. 7, p. 98.
8. H. Gelernter and J. C. Swihart, "A Mathematical-Physical Model of the Genesis of the Electrocardiogram," Biophys. J. 4, 285-301 (July 1964).
9. R. Plonsey, "An Extension of the Solid Angle Potential Formulation for an Active Cell," Biophys. J. 5, 663-667 (September 1965).